Cruise Report

GOOD-IMDOS

Le Commandant Charcot | Cruise No. CC220623

22.06.2023 - 10.07.2023

Reykjavik (Iceland) – Longyearbyen (Svalbard)

Andreas Oschlies[1], Aaron Beck[1], Kerstin Nachtigall[1], Deborah Stoll[1], Jan Taucher[1], Tim Boxhammer[1]

[1]GEOMAR Helmholtz Centre for Ocean Research Kiel

Table of content

Summary

1. Research program and objectives
    - 1.1 Work area
    - 1.2 Aims of the cruise
    - 1.3 Agenda of the cruise
2. Narrative of the cruise
    - 1.1 Narrative
    - 1.2 Sampling activities
3. Station list
4. Preliminary results
    - 4.1 Hydrography and oxygen concentration
        - 4.1.1 Methods
        - 4.1.2 Preliminary results
    - 4.2 Chlorophyll a and particulate matter
        - 4.1.1 Methods
        - 4.1.2 Preliminary results
    - 4.3 Mesozooplankton and particles
        - 4.3.1 Methods
        - 4.3.2 Preliminary results
    - 4.4 Microplastic distribution and composition
        - 4.4.1 Methods
        - 4.4.2 Preliminary results
    - 4.5 Science communication
        - 4.5.1 Popular science articles
5. Data availability
6. Science team
7. Acknowledgements
8. References

Summary

The cruise (CC220623) was part of an ongoing multi-year observation effort of the project GOOD-IMDOS (year 2 of 5) that is carried out in close cooperation with PONANT Science providing the ice breaker *Le Commandant Charcot (in short: Charcot)*, as a platform for opportunity science in the high Arctic. The project itself focuses on ongoing ocean deoxygenation as well as (micro-) plastic pollution in the Arctic. The cruise in 2023 consisted of just one leg from Reykjavik, Iceland (22 June 2023) to Longyearbyen, Svalbard (10 July 2023) and lasted a total of 19 days. The *Charcot,* a ship designed for extreme polar conditions, sailed from Reykjavik along the eastern coast of Greenland with intense sea ice coverage and crossed Fram Strait to reach Svalbard on July 2nd. The following 8 days the ship was operating in waters around Svalbard reaching up to 81° North, where sea ice coverage was entirely closed. With extraordinary support of the ship's crew and its captain, a total of 26 stations were sampled. Most stations were located in fjord systems or on the shelf, while three off-shelf deep-water stations covering the southward flowing East Greenland Current and the northward flowing West Spitsbergen Current have been investigated. CTD, dissolved oxygen, bulk particulate matter and optical Video Underwater Vision Profiler 6 (UVP6) measurements were taken. Whenever ice-free water was present at the stations, microplastic samples were obtained with a Manta Net. Macroplastic litter was collected on sea ice as well as on several beaches. Data are currently analyzed and will be used to better constrain models of marine oxygen dynamics and to form a database of microplastic distribution and composition in the Arctic. An improved understanding of oxygen dynamics in polar waters that source large parts of the deep ocean should help resolving the discrepancies between relatively low rates of deoxygenation in current climate models and considerably higher rates in observational estimates. The science team was accompanied by the professional photographer and videographer Xavier Boymond who documented the science activities on board. The collected footage has fed into several articles to raise awareness on the need for sustained and comprehensive in situ observations in the Arctic aiming to improve our knowledge of this highly remote area and to better predict its future changes.

1. Research program and objectives

1.1 Work area

Work area was the Atlantic sector of the Arctic Ocean, north of Iceland, along the eastern coast of Greenland, around Svalbard and in the closed sea ice coverage up to 81°N (Fig. 1).

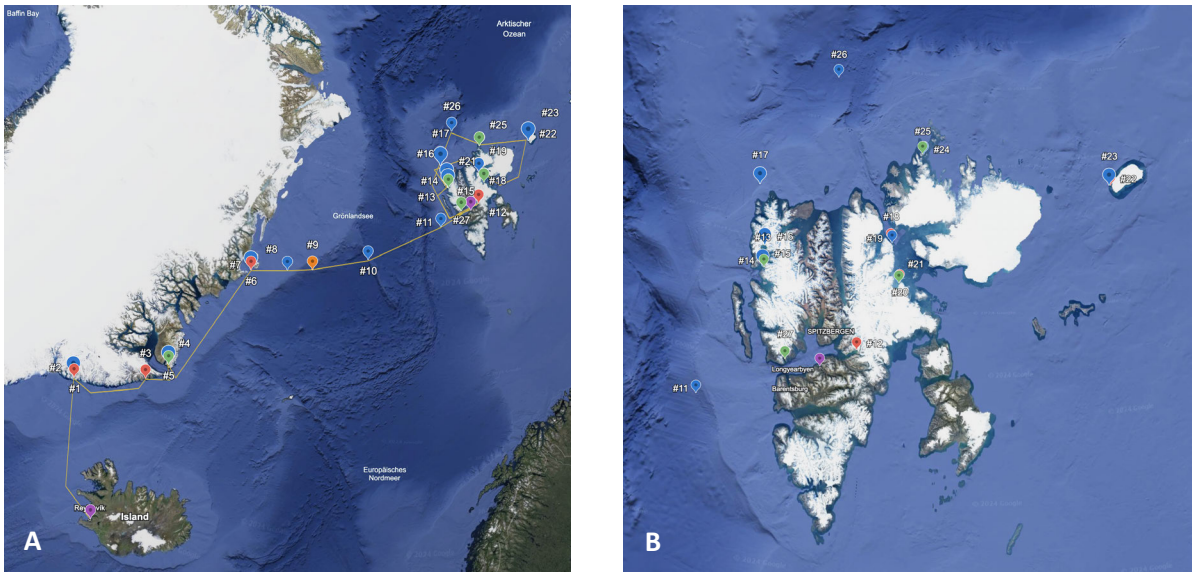

Fig. 1: Working area and sampling stations (#1 - #27) of the cruise CC220623 (A and B). Stations for water column sampling are highlighted in blue, those for microplastic in red and collections of macroplastic on sea ice and at beaches in green. Ports of Reykjavik and Longyearbyen are indicated in purple.

1.2 Aims of the cruise

Field work focused on the role of climate change and ocean pollution in the Atlantic sector of the Arctic Ocean, in particular on the extent and mechanisms of deoxygenation and microplastic pollution impacting the fragile marine ecosystems in the Arctic.

1.3 Agenda of the cruise

Measurements taken are a contribution to the UN Decade of Ocean Science for Sustainable Development endorsed program GOOD (Global Ocean Oxygen Decade), OARS (Ocean Acidification Research for Sustainability), and those of the Global Ocean Observing System (GOOS, here focusing on expanding global observations of marine litter as part of the Integrated Marine Debris Observing System, IMDOS). This cruise (CC220623) on *Le Commandant Charcot* (short: *Charcot*) was part of a

multi-year observation effort of the GOOD-IMDOS project (year 2 of 5) in close collaboration with PONANT Science.

2. Narrative of the cruise

2.1 Narrative

The cruise track covered a latitudinal gradient from 68°N (off Iceland) to 81°N (off Svalbard), in which most of the northward movement was along the Greenland coast (see Fig.1). Ice coverage was significantly below the mean sea ice extent in June / July of the reference period of 1981-2010 (National Snow and Ice Data Center) (Fig. 2). However, the *Charcot* traveled through largely intact sea ice and large fields of drifting ice sheets on its way North along the coast of Greenland to avoid swell from strong easterly winds. All stations sampled are visualized in Figure 1 and listed in full detail in Chapter 3 *Station List* (Table 3). Stations include those for water column sampling from the afterdeck as well as sea surface sampling from Zodiacs and manual collection of macroplastic on sea ice and beaches.

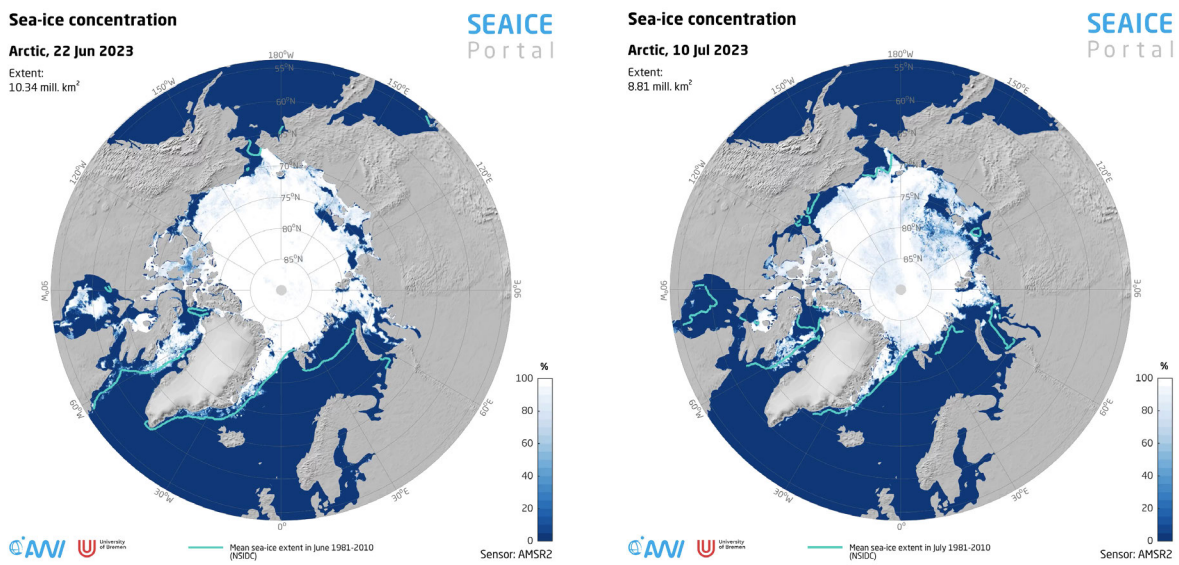

Fig. 2: Change of sea ice coverage and thickness over the course of the cruise (22 June 2023 - 10 July 2023). Sea ice data from www.meereisportal.de (funding: REKLIM-2013-04).

The *Charcot* left Reykjavik on 22 June 2023, crossing the Denmark Strait and entering the Nansen Fjord on 24 June 2023 without any stop for activities (see itinerary of the cruise in Table 1). First samples from the water column as well as from the ocean's surface were taken in Nansen Fjord (stations #1 &

#2). During the following days along the Blosseville Coast only one more station could be sampled (station #3) due to strong drift of ice sheets and high risk of losing irreplaceable equipment. On 27 June 2023 the ship reached the Greenland village Ittoqqortoormiit which allowed us to take samples from under the ice coverage enclosing the ship as well as collecting macroplastic on the ice nearby the village (stations #4 & #5). Further up the coast, again drifting sea ice prevented us from science activities until 29 June 2023 (stations #6 & #7). Crossing the Fram Strait from Greenland to Svalbard (30 June - 01 July 2023) we were able to do four more stops for sampling purposes (stations #8 - #11). However, station #9 had to be aborted after deploying the gear due to strong sea ice drift. Two off-shelf deep-water stations with sampling depth down to >700 m were successfully sampled (#10 & #11). The *Charcot* entered Isfjord (Svalbard) on 02 July 2023 allowing for another station to sample microplastic at the sea surface (#12). Reaching the fjord system of Krossfjord at the north west coast of Svalbard on 03 July 2023 we have been able to run another five stations (#13 - #17). From 04 to 05 July 2023 the *Charcot* sailed in the Hinlopen Strait with many stops giving us the chance to do serval water column as well as sea surface stations (#18 - #21). With Kvitøya Island the ship had reached the most eastern point of the cruise. Microplastic as well as water samples were taken off the coast of Kvitøya Island (#22 & #23). On 07 July 2023 the ship stopped in Nordenskiöld Bay allowing for further science activities including the manual collection of macroplastic on beaches (stations #24 & #25). The most northern point of the entire cruise was reached on 08 July 2023 at 81° North with fully closed sea ice coverage of the Arctic Ocean. The last sampling of the water column was conducted here (station #26). Before disembarkation on 10 July 2023, we had reached Isfjord again allowing for a last collection of macroplastic on a beach nearby Longyearbyen (station #27).

Table 1: Itinerary of the cruise (CC220623).

Date	**Area**
22 June 2023	Embarkation and departure in Reykjavik (Iceland)
23 June 2023	Transit the Denmark Straight
24 June 2023	Nansen Fjord (Greenland)
25 - 26 June 2023	Exploration along the Blosseville Coast (Greenland)
27 June 2023	Scoresby Sund / Ittoqqortoormiit (Greenland)
28 - 29 June 2023	Exploration of the North East of Greenland
30 June - 01 July 2023	Crossing the Fram Strait, enroute to Svalbard

02 July 2023	Isfjord (Svalbard)
03 July 2023	Krossfjord and north west of Svalbard
04 - 05 July 2023	Hinlopen Strait (Svalbard)
06 July 2023	Kvitøya Island
07 July 2023	Nordenskiöld Bay (Svalbard)
08 July 2023	81°N in fully closed sea ice coverage north of Svalbard
09 July 2023	Isfjord (Svalbard)
10 July 2023	Disembarkation in Longyearbyen (Svalbard)

2.2 Sampling activities

The sampling of the water column was performed from the afterdeck of the ship using a metal boom and a 1000 m rope that was marked every 5 - 50 m and operated with an electric winch originally used for the mooring lines. The boom ensured some distance of the instruments and samplers from the ship's hull. Taking vertical profiles and water samples from more than 800 m water depth took about 45 minutes. A professional CTD rosette as well as a dedicated winch will be installed in 2024 to allow for more efficient and professional sampling routines.

The CTD, the optical Underwater Vision Profiler 6 (UVP6-LP) as well as the Niskin bottles for water samples from discrete depths were deployed together to vertically resolved data of physical parameters (CTD), mesozooplankton and particles (UVP6-LP), as well as biogeochemical key parameters such as chlorophyll *a* and particulate carbon and nitrogen (Niskin, see Table 2). See chapters 4.1, 4.2 and 4.3 on *Hydrography and oxygen concentrations, Chlorophyll a and particulate matter* as well as *Mesozooplankton and particles* for further information on sampling, sample processing and analysis. Vertical profiles of the CTD and the UVP6-LP were always conducted to the maximum depth of the Niskin samples.

Microplastic sampling was carried out when ice-free water was present using a Manta Net that was towed behind a Zodiac (see Table 2). For more details on sampling and sample processing see chapter 4.4 on *Microplastic distribution and composition*.

Macroplastic sampling was done on sea ice off the village Ittoqqortoormiit as well as on several beaches with the support of the nature guides of PONTANT as well as several passengers (see Table

2). For more details on sampling and sample processing see chapter 4.4 on *Microplastic distribution and composition*.

Table 2: Parameters measured or sampled during the cruise.

Station type	**Parameter**	**Specifics**	**Person responsible**
Water column	Temperature, salinity, depth, oxygen (sensors)	CTD sensor (RBRmaestro³: multi-channel logger C.T.D.ODO.Tu|fast8|deep|wifi)	Tim Boxhammer
Water column	Mesozooplankton and particles (camera system)	Underwater Vision Profiler (Hydroptic UVP6-LP)	Tim Boxhammer
Water column	Particulate carbon and nitrogen (filtration)	Niskin bottle (0.5 - 1 L filtration volume)	Kerstin Nachtigall
Water column	Phytoplankton pigments (filtration)	Niskin bottle (0.5 - 1 L filtration volume)	Kerstin Nachtigall
Water column	O_2 (winkler)	Niskin bottle (0.3 L water volume)	Kerstin Nachtigall
Sea surface	Microplastic (filtration)	Manta Net (3 transects, 20 min each)	Deborah Stoll
Beaches Sea ice	Macroplastic (manual collection)	Manual collection by scientists, nature guides of PONANT and passengers	Deborah Stoll

In addition to the sampling activities several knowledge transfer activities for the passengers were carried out by the science team (Fig. 3).

Fig. 3: Passengers were involved in the ongoing research activities on board via talks (A), regular lab tours (B and C) and sampling of the water column (D).

Two talks, one at the beginning of the cruise and one at the end of the cruise, were given for the passengers on board to provide background information on science activities and to communicate preliminary findings. In addition, 8 lab tours and the opportunity to participate in sampling procedures on the afterdeck were offered to interested passengers.

3. Station list

In total 26 stations were sampled as one station (#9) needed to be aborted due to strong ice drift during the sampling process. This includes 13 CTD stations for vertical sensor profiles at shallow depth <100 m (6 stations), intermediate depth 100 - 300 m (4 stations) and at off the shelf locations 700 - 900 m (3 stations). Only in 8 cases vertical camera profiles were taken alongside the CTD. Water samples from discrete depths were taken at 9 of the 13 CTD stations. The sea surface was sampled for microplastic at in a total of 8 stations with 3 transects each.

Table 3: Station list of the cruise CC220623 providing detailed information: station ID, station type, precise information on date, time, position and water depth, sampling gear and the individual station features. Water column stations are highlighted in light blue, sea surface samplings for microplastic in light red and manual collection of macroplastic on ice or on beaches in light green.

ID	Type	Date and time	Position	Water depth	Sampling gear	Station features
#	open ocean, fjord, strait, under ice, on ice	dd.mm.yyyy hh:mm:ss CEST	00°00'00.00'' 00°00'00.00''	meters	CTD, UVP6, Niskin, Manta Net, manual collection	comments
1	fjord	24.06.2023 11:00:00	68°14'38.41'' N 29°38'13.10'' W	NA	Manta Net	rel. open water with some drift ice; 3 tracks
2	fjord	24.06.2023 18:40:00	68°17'38.69'' N 29°48'33.97'' W	300	CTD	afterdeck; test station; sanding dust (wood) in the air
2	fjord	24.06.2023 18:40:00	68°17'38.69'' N 29°48'33.97'' W	300	UVP	see CTD; UVP didn't take any pictures
2	fjord	24.06.2023 18:40:00	68°17'38.69'' N 29°48'33.97'' W	300	N7	see CTD

2	fjord	24.06.2023 18:40:00	68°17'38.69'' N 29°48'33.97'' W	300	N8	see CTD
3	fjord	26.06.2023 17:00:00	69°38'33.74'' N 23°26'15.95'' W	NA	Manta Net	3 tracks; ship left early; no water sampling possible due to drift ice
4	on ice	27.06.2023 12:00:00	70°28'37.53'' N 21°58'15.12'' W	0-30	manual collection	sampling of macroplastic on the sea ice surface from the ship's position to the Innuit village Ittoqqortoormiit
5	under ice	27.06.2023 16:00:00	70°28'37.53'' N 21°58'15.12'' W	30	CTD	under the ice next to the ship, 10m (seal hole)
5	under ice	27.06.2023 16:00:00	70°28'37.53'' N 21°58'15.12'' W	30	UVP	under the ice next to the ship, 10m (seal hole), many small particles (most likely resuspended sediments)
5	under ice	27.06.2023 16:00:00	70°28'37.53'' N 21°58'15.12'' W	30	N7	under the ice next to the ship, 10m (seal hole)
5	under ice	27.06.2023 16:00:00	70°28'37.53'' N 21°58'15.12'' W	30	N8	under the ice next to the ship, 10m (seal hole)
6	fjord	29.06.2023 11:00:00	74°48'28.13'' N 17°56'42.66'' W	300	CTD	afterdeck; rel. open water; ship drifting; water depth changed from 340-300m -> needed to adapt sampling depth and last Niskin during downcast
6	fjord	29.06.2023 11:00:00	74°48'28.13'' N 17°56'42.66'' W	300	UVP	see CTD; UVP was NOT pulled back to surface at the beginning but should have started to record at 5m water depth (according to the settings)
6	fjord	29.06.2023 11:00:00	74°48'28.13'' N 17°56'42.66'' W	300	N7	see CTD
6	fjord	29.06.2023 11:00:00	74°48'28.13'' N 17°56'42.66'' W	300	N6	see CTD
6	fjord	29.06.2023 11:00:00	74°48'28.13'' N 17°56'42.66'' W	300	N4	see CTD
6	fjord	29.06.2023 11:00:00	74°48'28.13'' N 17°56'42.66'' W	300	N3	see CTD

6	fjord	29.06.2023 11:00:00	74°48'28.13'' N 17°56'42.66'' W	300	N2	see CTD
7	fjord	29.06.2023 13:00:00	74°48'28.13'' N 17°56'42.66'' W	NA	Manta Net	rel. open and clean water; 3 tracks
8	open ocean	30.06.2023 11:00:00	75°17'36.00'' N 13°12'42.00'' W	225	CTD	afterdeck; open water with some drift ice; GPS coordinates from the bridge
8	open ocean	30.06.2023 11:00:00	75°17'36.00'' N 13°12'42.00'' W	225	UVP	see CTD; UVP was pulled back to surface at the beginning but depth profile starts at 5m water depth
8	open ocean	30.06.2023 11:00:00	75°17'36.00'' N 13°12'42.00'' W	225	N8	see CTD
8	open ocean	30.06.2023 11:00:00	75°17'36.00'' N 13°12'42.00'' W	225	N7	see CTD
8	open ocean	30.06.2023 11:00:00	75°17'36.00'' N 13°12'42.00'' W	225	N5	see CTD
8	open ocean	30.06.2023 11:00:00	75°17'36.00'' N 13°12'42.00'' W	225	N4	see CTD
8	open ocean	30.06.2023 11:00:00	75°17'36.00'' N 13°12'42.00'' W	225	N3	see CTD
8	open ocean	30.06.2023 11:00:00	75°17'36.00'' N 13°12'42.00'' W	225	N2	see CTD
9	open ocean	30.06.2023 20:00:00	75°35'12.40'' N 09°46'59.00'' W	1800	CTD, UPV, Niskin	CANCELED after CTD and camera were already in the water - TOO MUCH DRIFT ICE
10	open ocean	01.07.2023 10:00:00	76°23'22.95'' N 01°53'20.37'' W	3400	CTD	afterdeck; right after the ice edge;
10	open ocean	01.07.2023 10:00:00	76°23'22.95'' N 01°53'20.37'' W	3400	UVP	see CTD
10	open ocean	01.07.2023 10:00:00	76°23'22.95'' N 01°53'20.37'' W	3400	N8	see CTD
10	open ocean	01.07.2023 10:00:00	76°23'22.95'' N 01°53'20.37'' W	3400	N7	see CTD

10	open ocean	01.07.2023 10:00:00	76°23'22.95'' N 01°53'20.37'' W	3400	N6	see CTD
10	open ocean	01.07.2023 10:00:00	76°23'22.95'' N 01°53'20.37'' W	3400	N5	see CTD
10	open ocean	01.07.2023 10:00:00	76°23'22.95'' N 01°53'20.37'' W	3400	N4	see CTD
10	open ocean	01.07.2023 10:00:00	76°23'22.95'' N 01°53'20.37'' W	3400	N3	see CTD
10	open ocean	01.07.2023 10:00:00	76°23'22.95'' N 01°53'20.37'' W	3400	N2	see CTD
11	open ocean	02.07.2023 02:30:00	77°43'19.31'' N 09°55'13.53'' E	1000	CTD	afterdeck; no ice in sight; line did not go down vertically; very fast downcast (little time window)
11	open ocean	02.07.2023 02:30:00	77°43'19.31'' N 09°55'13.53'' E	1000	UVP	see CTD
11	open ocean	02.07.2023 02:30:00	77°43'19.31'' N 09°55'13.53'' E	1000	N8	see CTD; accidently opened during transport!
11	open ocean	02.07.2023 02:30:00	77°43'19.31'' N 09°55'13.53'' E	1000	N7	see CTD
11	open ocean	02.07.2023 02:30:00	77°43'19.31'' N 09°55'13.53'' E	1000	N6	see CTD
11	open ocean	02.07.2023 02:30:00	77°43'19.31'' N 09°55'13.53'' E	1000	N5	see CTD
11	open ocean	02.07.2023 02:30:00	77°43'19.31'' N 09°55'13.53'' E	1000	N4	see CTD
11	open ocean	02.07.2023 02:30:00	77°43'19.31'' N 09°55'13.53'' E	1000	N3	see CTD
11	open ocean	02.07.2023 02:30:00	77°43'19.31'' N 09°55'13.53'' E	1000	N2	see CTD
12	fjord	02.07.2023 15:00:00	78°26'36.17'' N 17°20'38.90'' E	NA	Manta Net	glacier runoff with brown water; three tracks

13	fjord	03.07.2023 09:00:00	79°07'34.42'' N 11°48'43.96'' E	55	CTD	afterdeck; manually; very milky water; no stratification; no water samples for filtration; no camera used
14	beach	03.07.2023 10:00:00	79°07'31.00''N 11°52'39.00'' E	0	manual collection	lots of plastic on the beach called "14th July", between 79°07'31.00'' N 11°52'39.00'' E and 79°07'37.30''N 11°51'52.70''E
15	fjord	03.07.2023 14:00:00	79°20'38.62'' N 11°41'11.25'' E	NA	Manta Net	glacier front; three tracks; slightly milky water
16	fjord	03.07.2023 16:00:00	79°20'38.62'' N 11°41'11.25'' E	100	CTD	from the Zodiac; glacier front
17	open ocean	04.07.2023 00:30:00	79°56'27.60" N 10°40'15.60" E	340	CTD	afterdeck; northwest end of Svalbard; strong currents; line relatively vertical
17	open ocean	04.07.2023 00:30:00	79°56'27.60" N 10°40'15.60" E	340	UVP	many copepods and appendicularian houses!
17	open ocean	04.07.2023 00:30:00	79°56'27.60" N 10°40'15.60" E	340	N8	see CTD
17	open ocean	04.07.2023 00:30:00	79°56'27.60" N 10°40'15.60" E	340	N7	see CTD
17	open ocean	04.07.2023 00:30:00	79°56'27.60" N 10°40'15.60" E	340	N6	see CTD
17	open ocean	04.07.2023 00:30:00	79°56'27.60" N 10°40'15.60" E	340	N5	see CTD
17	open ocean	04.07.2023 00:30:00	79°56'27.60" N 10°40'15.60" E	340	N4	see CTD
17	open ocean	04.07.2023 00:30:00	79°56'27.60" N 10°40'15.60" E	340	N3	see CTD
17	open ocean	04.07.2023 00:30:00	79°56'27.60" N 10°40'15.60" E	340	N2	see CTD

18	strait	04.07.2023 13:00:00	79°34'32.78'' N 18°34'18.40'' E	NA	Manta Net	guillemot breeding area (1+ Mio birds); 3 tracks along the coast line (position = start of 2nd track), (ship position = 79°34'04.47'' N 18°41'07.12'' E)
19	strait	04.07.2023 16:00:00	79°33'32.82'' N 18°38'35.39'' E	170	CTD	CTD relatively close to shore; small glacier run off; BY HAND from Zodiac - therefore no Niskin; relatively close to the bird colony (ship position = 79°34'04.47'' N 18°41'07.12'' E)
20	fjord	05.07.2023 15:00:00	79°10'05.16'' N 19°14'33.58'' E	NA	Manta Net	close to the glacier front; rel. open water; 3 tracks (position = start of 2nd track), (ship position = 79°09'38.43'' N 19°10'42.40'' E)
21	beach	05.07.2023 15:00:00	79°09'25.98'' N 19°12'16,56'' E	0	manual collection	Macroplastic collection by the naturalists of PONANT
22	open ocean	06.07.2023 09:00:00	80°06'45.11'' N 31°23'31.85'' E	NA	Manta Net	close to shore of Kvitøya island; 3 tracks (position = start of 2nd track), (ship position = 80°06'36.00'' N 31°18'47.99'' E)
23	open ocean	06.07.2023 10:30:00	80°06'39.14'' N 31°18'43.89'' E	65	CTD	CTD from Zodiac (Zodiac position); relatively open water; CTD station during the night was canceled; CTD from the after deck impossible due to ship and ice movement (ship position = 80°06'36.00'' N 31°18'47.99'' E)
24	fjord	07.07.2023 14:30:00	80°29'16.49'' N 20°05'57.35'' E	100	CTD	afterdeck; no wind; partly ice free; drift ice not moving; very little propeller movement
24	fjord	07.07.2023 14:30:00	80°29'16.49'' N 20°05'57.35'' E	100	UVP	see CTD
24	fjord	07.07.2023 14:30:00	80°29'16.49'' N 20°05'57.35'' E	100	N7	see CTD
24	fjord	07.07.2023 14:30:00	80°29'16.49'' N 20°05'57.35'' E	100	N6	see CTD

24	fjord	07.07.2023 14:30:00	80°29'16.49'' N 20°05'57.35'' E	100	N4	see CTD
24	fjord	07.07.2023 14:30:00	80°29'16.49'' N 20°05'57.35'' E	100	N2	see CTD
25	beach	07.07.2023 16:00:00	80°29'17.99'' N 20°06'29.99'' E	0	manual collection	macroplastic collection on the beach (by the guides of CC)
26	open ocean	08.07.2023 14:30:00	81°10'16.52'' N 14°08'44.79'' E	1400	CTD	afterdeck; ocean fully covered with ice;
26	open ocean	08.07.2023 14:30:00	81°10'16.52'' N 14°08'44.79'' E	1400	UVP	see CTD
26	open ocean	08.07.2023 14:30:00	81°10'16.52'' N 14°08'44.79'' E	1400	N7	see CTD
26	open ocean	08.07.2023 14:30:00	81°10'16.52'' N 14°08'44.79'' E	1400	N5	see CTD
26	open ocean	08.07.2023 14:30:00	81°10'16.52'' N 14°08'44.79'' E	1400	N4	see CTD
26	open ocean	08.07.2023 14:30:00	81°10'16.52'' N 14°08'44.79'' E	1400	N3	see CTD
26	open ocean	08.07.2023 14:30:00	81°10'16.52'' N 14°08'44.79'' E	1400	N2	see CTD
27	beach	09.07.2023 16:00:00	78°15'01.78'' N 13°50'20.76'' E	0	manual collection	Macroplastic collection by team and naturalists of PONANT in the fjord system around Longyearbyen

4. Preliminary Results

4.1 Hydrography and oxygen concentration

4.1.1 Methods

In total 13 CTD casts were performed at different locations during the cruise (Tab. 3) using a RBRmaestro³ multi-channel logger (C.T.D.ODO.Tu|fast8|deep|wifi) equipped with a pre-calibrated

RBR*coda*T.ODO|fast oxygen sensor. Six casts were located at very shallow stations down to <100 m water depth (usually in fjord systems close to shore), four at intermediate depth stations of 100 - 300 m water depth (over the shelf) and three at off-shelf deep-water stations allowing CTD casts down to 700 - 900 m (Fig. 1). The deep-water stations covered the southward flowing East Greenland Current as well as the northward flowing West Spitsbergen Current. Most CTD casts were taken from the afterdeck of *Charcot*, using the pre-installed 1000 m sampling line and the winch (Fig. 4 A and B). In this case also water samples from discrete depth were taken with so called Niskin bottles for manual measurements of oxygen on board. The Niskin bottles were attached to the sampling line in pre-defined distances. Being open on the way down to the desired depth, the bottles were closed remotely using so called messenger weights. In four cases, the CTD profiles were taken from the Zodiac without taking additional water samples (Tab. 3). Only in one case, the CTD and Niskin bottles were operated manually, standing on the closed sea ice coverage next to *Charcot* and lowering the equipment through a seal hole in the ice (station #5). The vertical sensor profiles of the CTD include the following parameters: Temperature, salinity, oxygen concentration and calculated oxygen saturation. CTD data were only used from the downward cast since the instrument has no pump to supply the sensors mounted at the bottom with a constant waterflow. Absolute oxygen concentrations at discrete depths were measured of triplicate samples taken from the Niskin samplers using the Winkler O_2 titration method as described in Arístegui and Harrison (2002). The water samples for analysis were taken bubble free in glass bottles allowing significant overflow and were closed airtight without any headspace (Fig. 4 D). The manually measured oxygen concentrations will help to verify and calibrate the sensor-based oxygen data.

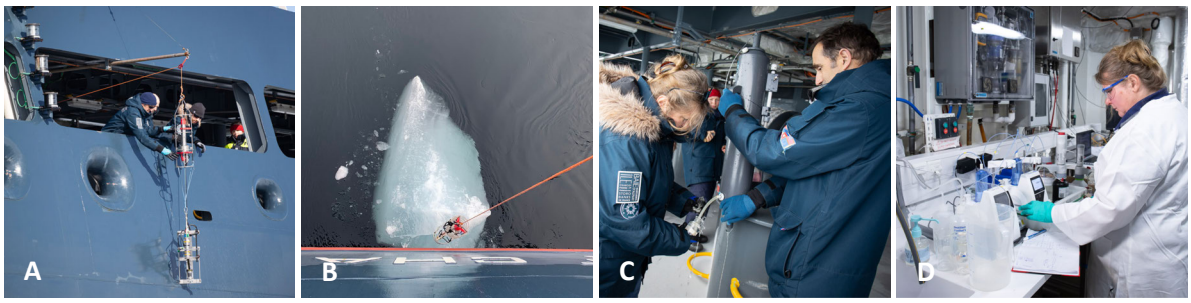

Fig. 4: CTD operation from the afterdeck of the ship (A and B) as well as sampling of water masses from discrete depths (C) for manual determination of oxygen concentrations in the lab (D). Photo credit: Xavier Boymond.

4.1.2 Preliminary results

The first CTD profile of interest is the one of station #5 located in the Scoresby Sund (Greenland) off the coast of the village Ittoqqortoormiit. Meltwater from snowfields and glaciers nearby had formed

a freshwater lens below the sea ice of 2 m thickness, visible from the salinity gradient of 0 to 32 PSU and the temperature gradient from 2 to -1°C within this layer (Fig. 5).

A general pattern observed was the oxygen undersaturation in waters off the coast of Greenland (Fig. 5, stations #5 - #8). The first station showing oxygen oversaturation at the surface (upper 20 m) is station #10, located in the East Greenland Current between Greenland and Svalbard (Fig. 6).

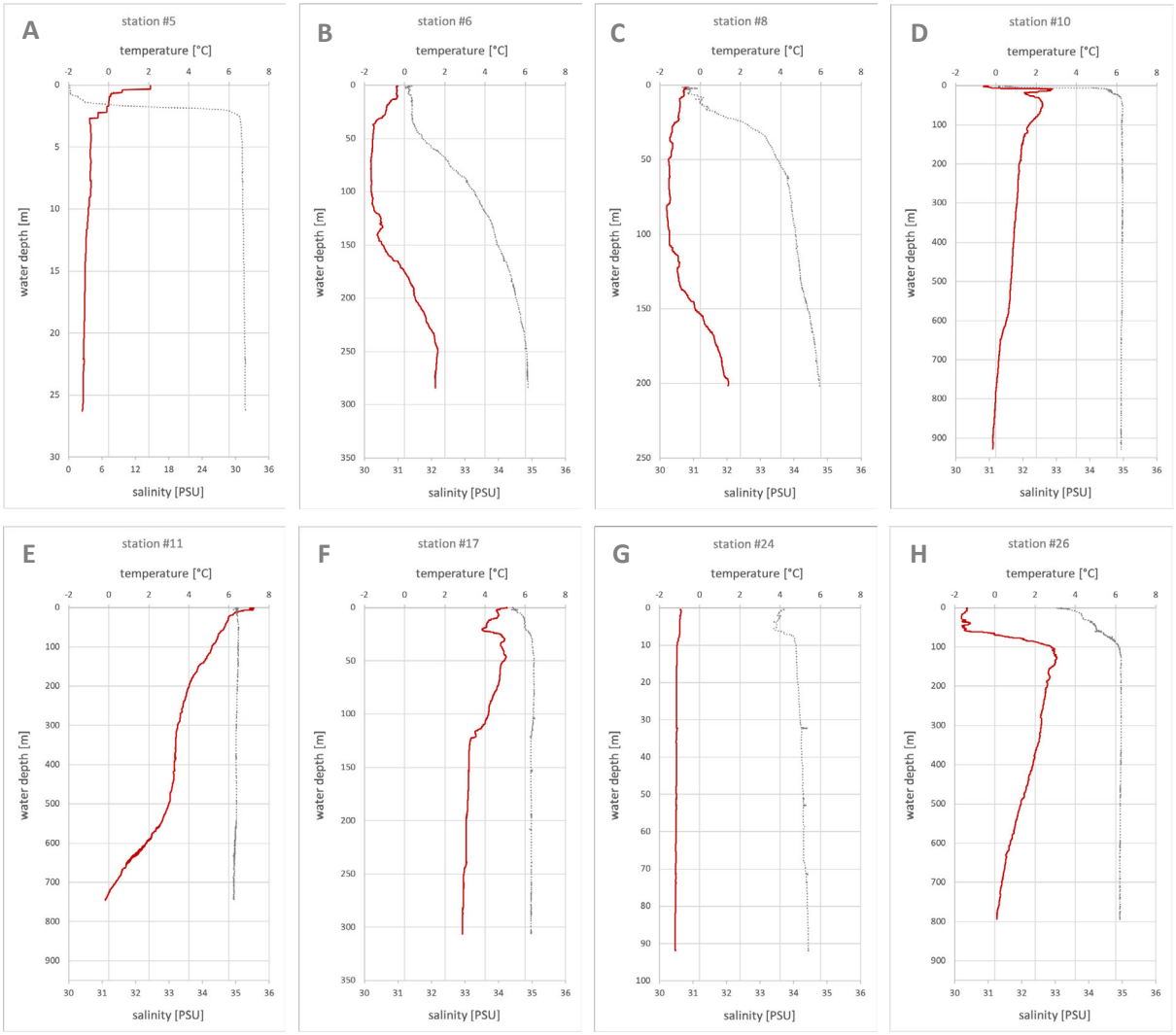

Fig. 5: Vertical CTD profiles of temperature and salinity of selected stations covering the coast of Greenland (stations #5 - #8), the transect to Svalbard (stations #10 and #11), the Svalbard archipelago (stations #17 and #24) and the closed sea ice coverage north of Svalbard at 81°N (station #26). See Fig. 1 and Table 3 for the exact position of each station. The red solid lines represent the sea water temperature in degrees Celsius, while the grey dotted line represent the salinity. The scale of the Y-axis varies depending on the sampling depths of the individual stations.

All stations around the Svalbard archipelago showed an oversaturation of oxygen in the upper 20 m (Fig. 6, stations #11 - #26). Station # 11 was located in the West Spitsbergen Current, characterized by

a relatively high salinity >35 PSU (Fig. 5), the warmest water temperatures of the entire cruise and the strongest temperature gradient ranging from 7°C at the sea surface to <0°C at 750 m water depth.

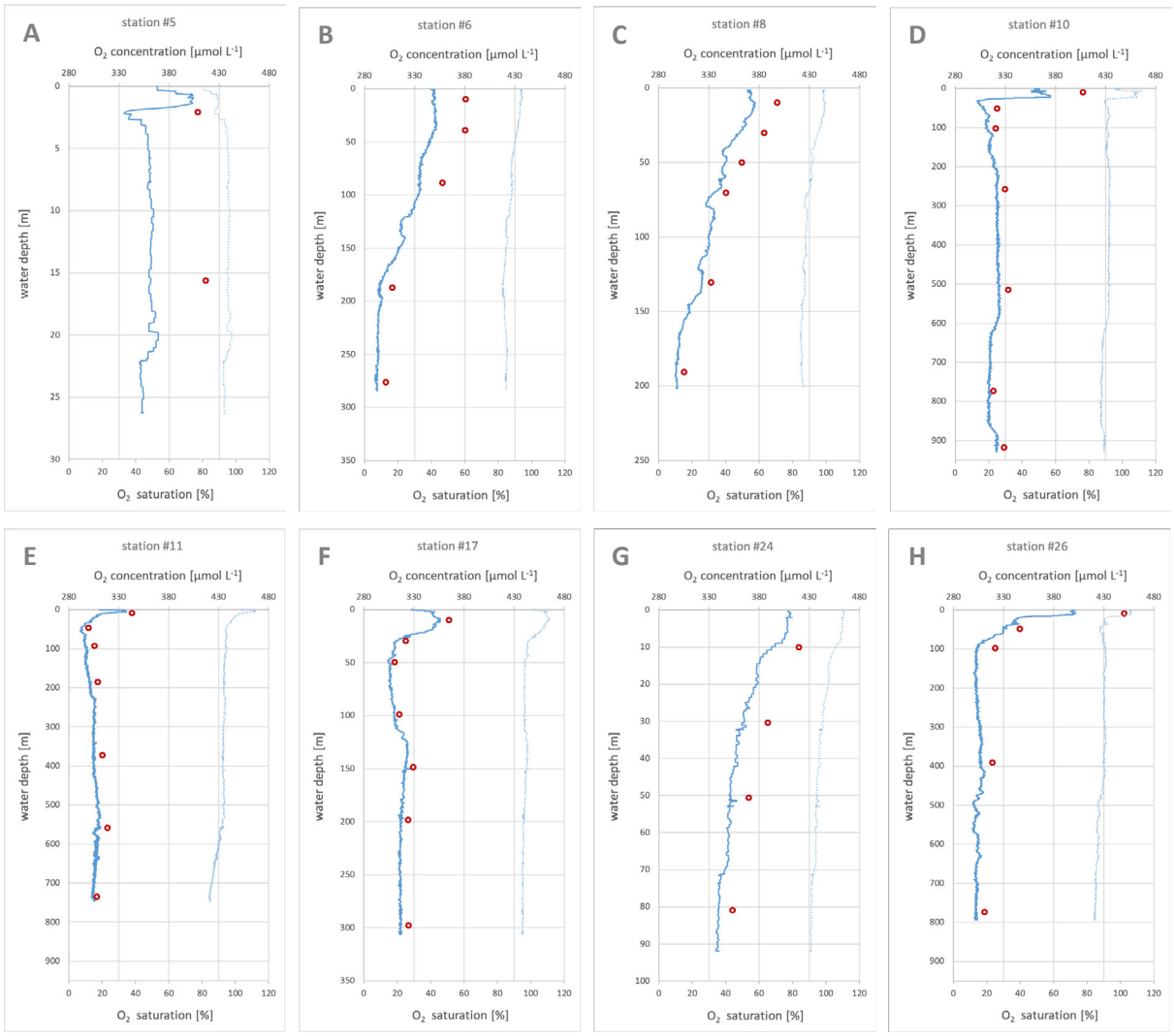

Fig. 6: Vertical CTD profiles of oxygen concentration and oxygen saturation of selected stations covering the coast of Greenland (stations #5 and #6), the transect to Svalbard (stations #8 - #11), the Svalbard archipelago (stations #17 and #24) and the closed sea ice coverage north of Svalbard at 81°N (station #26). See Fig. 1 and Table 3 for the exact position of each station. The blue solid lines represent the oxygen concentration in µmol L^{-1}, dotted blue lines the oxygen saturation in percent, while the red circles represent manual oxygen measurements of samples taken from discrete depths. The scale of the Y-axis varies depending on the sampling depths of the individual stations.

This water mass represents the highly saline and still relatively warm water coming from the Gulf Stream to reach the high Arctic, where the water cools down to slowly start sinking with increasing density. This so-called deep-water formation is essential for transportation of oxygen to the deep ocean and the reason why it is so crucial to collect more biogeochemical data in this ocean region. The strongest oxygen gradient was observed at the most northern station (#26) where *Charcot* stopped in fully closed sea ice at 81°N.

Here, the oxygen level dropped from >400 µmol L^{-1} down to <300 µmol L^{-1} within the upper 100 m of the water column. Also, oxygen oversaturation was high at this station with 111% at the sea surface. The strong gradient is most likely a result of the different water layers obvious from the temperature and salinity gradients (Fig. 5, station #26). Both temperature and salinity reveal a cooler and less saline water layer down to 100 m water depths underneath the sea ice with a strong gradient of about 4°C and almost 2 PSU.

The highly precise measurement of oxygen concentration using the Winkler method revealed an offset in almost all oxygen profiles measured with the CTD oxygen sensor. Frequent re-calibration of this sensor is therefore crucial for accurate oxygen data in the future.

At most stations the propellers of the ship were in used to keep *Charcot* perfectly in position. However, the movement of the propellers has an impact on the mixing of approx. the upper 20 m of the water column. Unfortunately, the impact of this artifact on measured data close to sea surface remains unclear.

4.2 Chlorophyll *a* and particulate matter

4.2.1 Methods

Concentrations of Chlorophyll *a* and particulate matter (PM) were analyzed from subsamples taken from the Niskin bottles, filled at discrete depths as described in chapter 4.1.1 (Fig. 7 A-C). Subsamples were filtered onto pre-combusted (450 °C, 6 h) glass-fiber filters (GF/F, 0.7 µm nominal pore size, Whatman) applying a gentle vacuum of 200 mbar (Fig. 7D).

Fig. 7: Sampling of water masses from discrete depths from the afterdeck using Niskin bottles (A-C) for filtration in the lab (D) to determine phytoplankton pigments as well as particulate carbon and nitrogen concentrations. Photo credit: Xavier Boymond.

The filtration volumes varied between 500 - 1000 mL depending on the variable amount of particulate material present in the samples. Filters were stored in in cryo vials at -80 °C on board of the ship before

transportation to Germany on dry ice. Total particulate carbon (TPC) and nitrogen (TPN) was analyzed at GEOMAR (Germany) following Sharp (1974). The frozen pigment samples (Chlorophyll *a*) were stored at -80 °C until extraction as described by Paul et al. (2015). Concentrations of extracted pigments were measured by means of reverse-phase high-performance liquid chromatography (HPLC; Barlow et al., 1997) calibrated with commercial standards.

4.2.2 Preliminary results

Chlorophyll *a* (Chl *a*) concentrations were rather low, but variable, ranging between approx. 0.1 to 2.5 µg L^{-1} (Fig. 7A). Highest concentrations were reached in the upper 50 m of the water column (Fig. 8E) with some elevated values at intermediate depths indicate sinking of fresh phytodetritus (Fig. 8A).

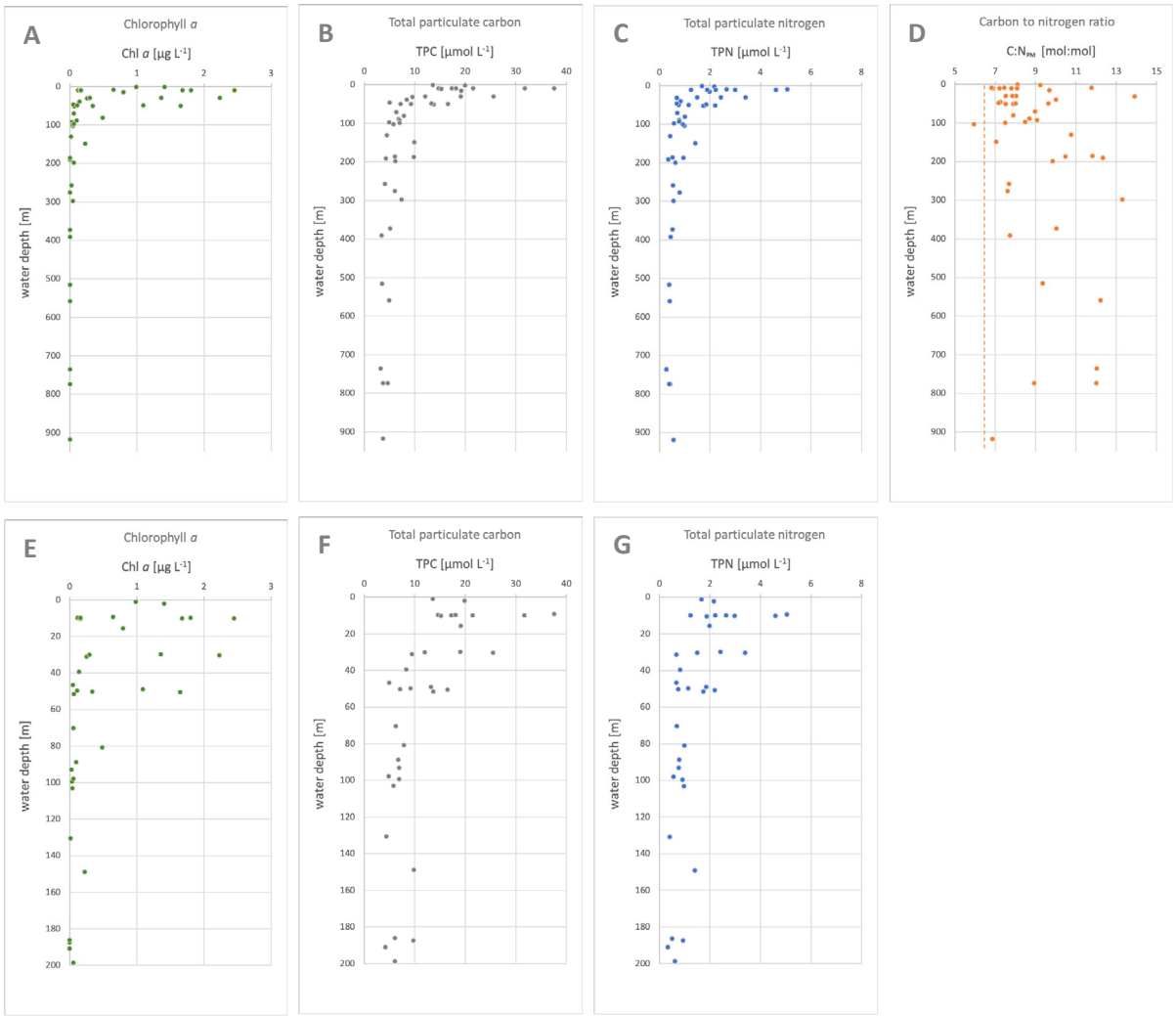

Fig. 8: Vertical profiles of Chlorophyll *a* (Chl *a*) (A and E), total particulate carbon (TPC) (B and F), total particulate nitrogen (TPN) (C and G), as well as the carbon to nitrogen ratio (C:N) of particulate matter (PM) (D) of all stations. Green dots represent the Chl *a* concentration in µg L^{-1}, grey dots the one of total particulate carbon (TPC) in µmol L^{-1}, while blue dots

represent the concentration of total particulate nitrogen in µmol L^{-1}. Orange dots represent C:N of particulate matter as a molar ratio, with the Redfield ration of C:N is indicated by the orange dotted line.

Total particulate carbon (TPC) concentrations displayed the typical exponential decrease with depth (Fig. 8B and F), decreasing from maximum values of almost 40 µmol C L^{-1} near the surface to values well below 10 µmol L^{-1} at depths >50m. Notably, molar carbon to nitrogen ratios (C:N) were elevated compared to the canonical Redfield ratio of 6.6 (Fig. 8D) . The average C:N ratio of all samples was 8.98, and the highest frequency was found between 7 and 9. There was no relationship between C:N and depth, which would indicate preferential remineralization of nitrogen over carbon.

4.3 Mesozooplankton and particles

4.3.1 Methods

The Underwater Vision Profiler 6 (UVP6-LP) is a special underwater camera system that collects images of particles and plankton during vertical profiles (Picheral et al. 2021). The UVP6-LP captured images at ~10 Hz with a pixel resolution of 73 µm in an imaged volume of ~600 ml, thus allowing to image and identify particles of organisms between approx. 1 to 100 mm (Fig. 9).

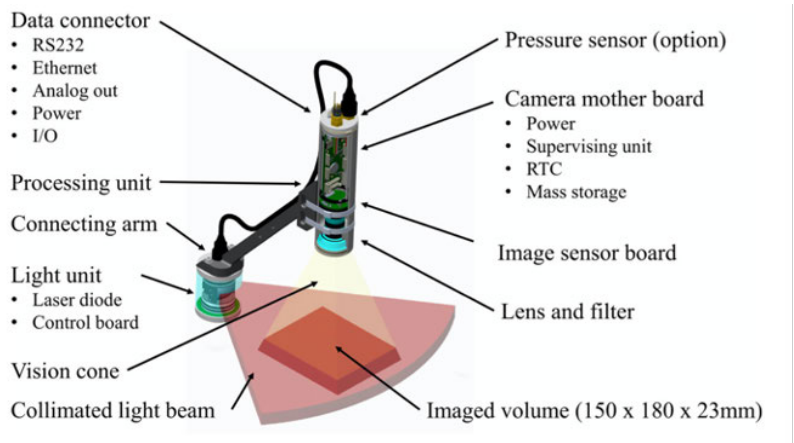

Fig. 9: Diagram of the UVP6-LP underwater camera. Credit: Hydroptic

Collected data were processed with the UVPapp software (provided by the manufacturer Hydroptic), including automated segmentation of “regions of interests” from raw images, and estimating their size (based on the number of pixels and geometric calculations). The software also provides vertical profiles of different size classes of particles captured with the UVP6-LP (Fig. 10).

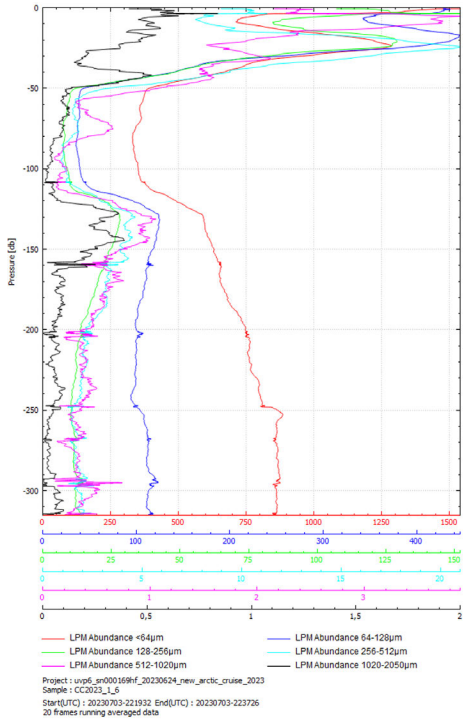

Fig. 10: Vertical profiles of different size classes of particles captured with the UVP6-LP at station #17 off the northwestern coast of Svalbard.

The UVP6-LP was usually operated together with the CTD using the 1000 m sampling line and the winch on the afterdeck of *Charcot* to collect vertically resolved data (Fig. 11). However, in one case (station #5) the camera system was manually operated under the closed ice coverage next to the ship.

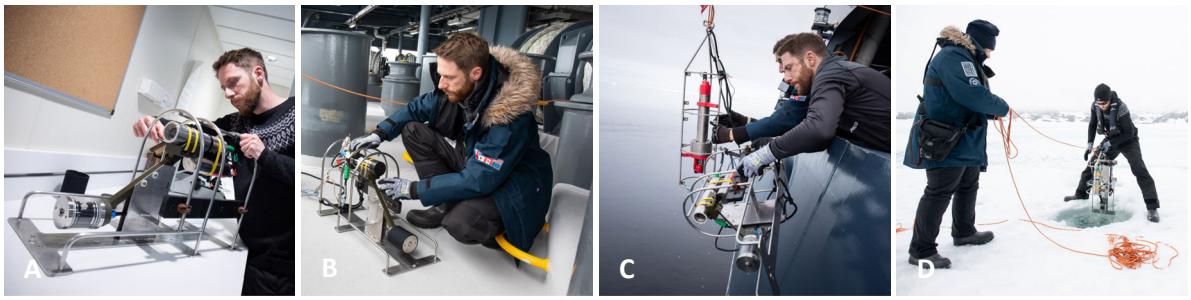

Fig. 11: Preparation (A) and operation of the UVP6-LP camera system at the afterdeck of *Charcot* (B and C) as well as under sea ice (D). Photo credit: Xavier Boymond.

4.3.2 Preliminary results

Presently, data analysis is in early phase, including classification of all detected organisms into taxonomic groups, and estimating their biovolume and its vertical profiles in the water column. Final

data should be available in summer 2024 and provided on the “EcoTaxa” platform, a plankton imaging database that collects data from all UVP units and provides them to the scientific community.

Preliminary analysis of data suggests very similar patterns of mesozooplankton abundance and taxonomic composition as observed during the cruise in 2022 (O030622). A distinct spatial gradient in zooplankton abundance and taxonomic composition, with higher copepod abundances in southern stations, and lower overall abundances at more northern stations (including a shift from copepods to gelatinous taxa such as appendicularia had already been observed in 2022 (see typical picture in Fig. 12). This pattern was likely related to seasonality i.e. particularly sea ice coverage, strongly effecting primary production and thereby the food source of mesozooplankton: Stations along the East Greenland shelf were still subject to a semi-closed sea ice coverage or large floating ice sheets leaving only little space for the sun to penetrate into the water column and to induce phytoplankton production.

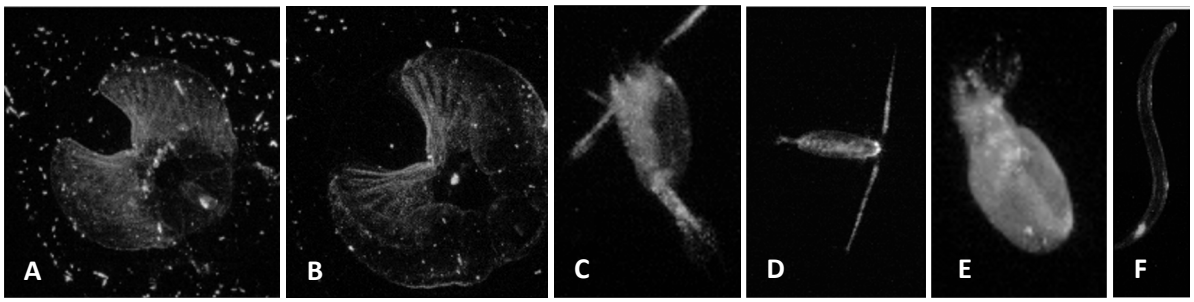

Fig. 12: Pictures of mesozooplankton individuals taken by the UVP6-LP during the vertical casts. Appendicularians (A and B), copepods (C-D), unknown species (E) and a pelagic living worm (F).

4.4 Microplastic distribution and composition

4.4.1 Methods

Sample collection

Microplastic (MP) was sampled from the sea surface with a Manta Net (mesh size 300 µm, opening 20 x 60 cm) deployed from a Zodiac (Fig. 13A and B). The net was fixed on a lateral boom to maintain space between boat and the net. Triplicates were taken at each station, considering the patchy distribution of MP and to provide a representative coverage of the site. At each station, three net tows were conducted for 20 min at a speed of ca. 4 knots, covering an area of about 1483 m^2 or a tow length of up to 2472 m. To keep track of position and tow length, a GPS device continuously recorded during the sampling process. Everything collected in the net was washed into the cod end after each transect. The cod end was replaced and stored in a stainless-steel container with a tight fitting lid. In the ship’s

laboratory, microplastic particles were rinsed from the cod ends into stainless-steel 300 µm sieves and carefully transferred into 500 ml swing-top glass jars (Fig. 13 C). MP particles were collected with tweezers from the glass jars into tightly closed petri dishes and visually identified under a microscope (Evident Olympus, Tokyo, Japan) (Fig. 13 D). A total of 8 stations were sampled, collecting 24 net tow samples (see station list in Table 3). MP samples were stored in labeled and tightly closed petri dishes. Samples were transported back to the laboratory at GEOMAR (Germany) for polymer analysis.

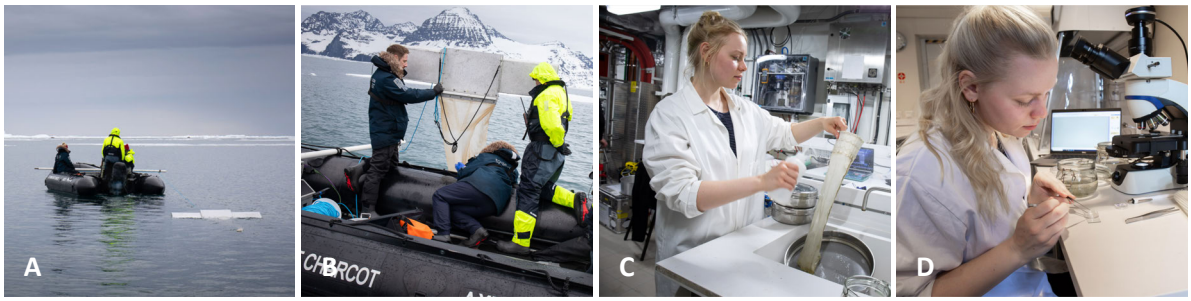

Fig. 13: Micro plastic sampling with the Manta Net (A and B) and processing of the sample material in the lab (C and D). Photo credit: Xavier Boymond.

Macroplastic litter (Fig. 14) was collected manually at various locations, e.g., near the village of Ittoqqortoormiit and the Svalbard shoreline. A total of 5 macroplastic stations were sampled with the help of the naturalist guides as well as passengers (see station list in Table 3). Big macroplastic pieces were subsampled (ca. 0.5 cm^2). Macroplastic subsamples were stored individually in labeled, tightly-closed petri dishes and transported back to GEOMAR (Germany) for polymer identification.

Fig. 14: Macroplastic samples collected on sea ice (A) as well as on beaches (B-D). Photo credit: Tim Boxhammer.

Polymer analysis

The polymer types of suspected microplastics were identified using a near-infrared hyperspectral camera system (NIR-HSI; Beck et al., 2023). The hyperspectral imaging system used in the current study was a Specim FX17 camera (Specim Spectral Imaging Ltd.; Oulu, Finland) mounted on a Specim linear lab bed scanner. The FX17 linescan camera has a spectral range of 900 – 1700 nm, with 224 spectral bands and spatial sampling of 640 pixels. A macro lens was used to achieve a field of view of

about 1200 µm, giving a pixel dimension of approximately 2 – 4 µm. Particles were mounted on a black, non-reflective slide and illuminated overhead by two halogen lights at approximately 45°C from the front and back of the camera target field. The hyperspectral camera and lab scanner were controlled using Specim's LUMO software suite. A combination of an edge-finding algorithm (Sobol) and a segmentation algorithm (Watershed) from Scikit-image (van der Walt et al., 2014), were used to identify particles in the images. Particle dimensions were calculated according to the calibrated pixel size. NIR spectra were averaged over the identified particle area. The Scikit-learn random forest algorithm (Pedregosa et al., 2011) was used to classify the particle polymer types based on this average spectral signature. The algorithm was trained and validated using plastic polymer standards produced in the BASEMAN project (Gerdts, 2017). The polymers in the training set included polystyrene (PS), polyvinyl chloride (PVC), high- and low-density polyethylene (HDPE and LDPE), polyethylene terephthalate (PET), and polypropylene (PP). Polyethylene was grouped as a single type because the NIR spectra for high- and low-density PE are identical. The spectra for plastic polymers are markedly different from those for natural materials.

4.4.2 Preliminary results

Microplastic was found in 21 of the 24 individual net tows and at all 8 Stations (Fig. 15). Microplastic abundance varied widely from 3 MP particles / tow (Greenland coast) up to 92 MP particles / tow (Svalbard). The high variability was not only present throughout the stations but also within the stations' individual net tows. For example, at Station #7 (net tows 16 to 18) 4, 10 and 78 MP were collected in each of the triplicate tows.

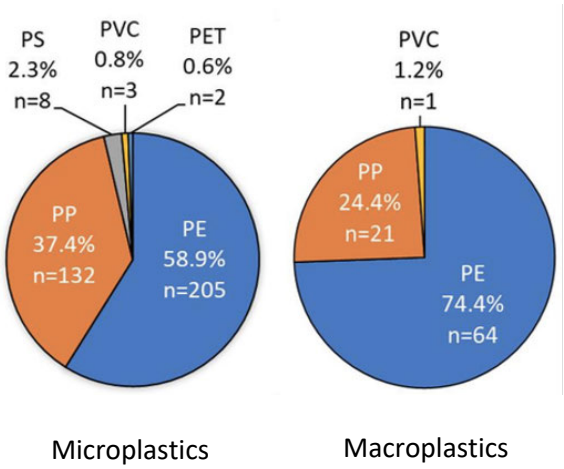

Fig. 15: Microplastic and macroplastic particles collected in 2023. Proportion of polymer types detected in the net collected microplastic particles and microplastic debris collected from shore. "n" indicates the total number of particles of each type.

This can be explained by the irregular distribution of MP particles, as mentioned earlier, and the sampling method aiming to provide representative data of each site more than taking replicates in a strict sense. The distribution of MP-particles at each site is also highly influenced by currents and windrows (Thorpe, 2009; Hamner and Schneider, 1986; Van Sebille et al., 2020) and can fluctuate in less time than needed for one net tow (Thorpe, 2009). A much higher MP concentration was observed when the net tow path crossed such an accumulation of particles.

Among the MP particles collected via manta net, PE (87%) was the most abundant polymer type, followed by PP (12%), with PA66 being the least abundant, representing only 1% (Fig. 3). Since PE and PP are known to have a density lower than sea water (<1.037 g/cm^3), the high prevalence of these polymers is not surprising. PE (69%) and PP (30%) were also the most abundant polymer types detected in local macroplastic debris sampled along the shorelines of Greenland and Svalbard. These results suggest local macroplastics fragmentation may be the main source of microplastic particles in the investigated area.

We have visualized the spatial distribution of MP, showing that MP were found at all stations in 2023 (Fig. 16). It is visible that MP were found even in the most remote sampling sites.

Microplastic in Greenland and Svalbard (2023)

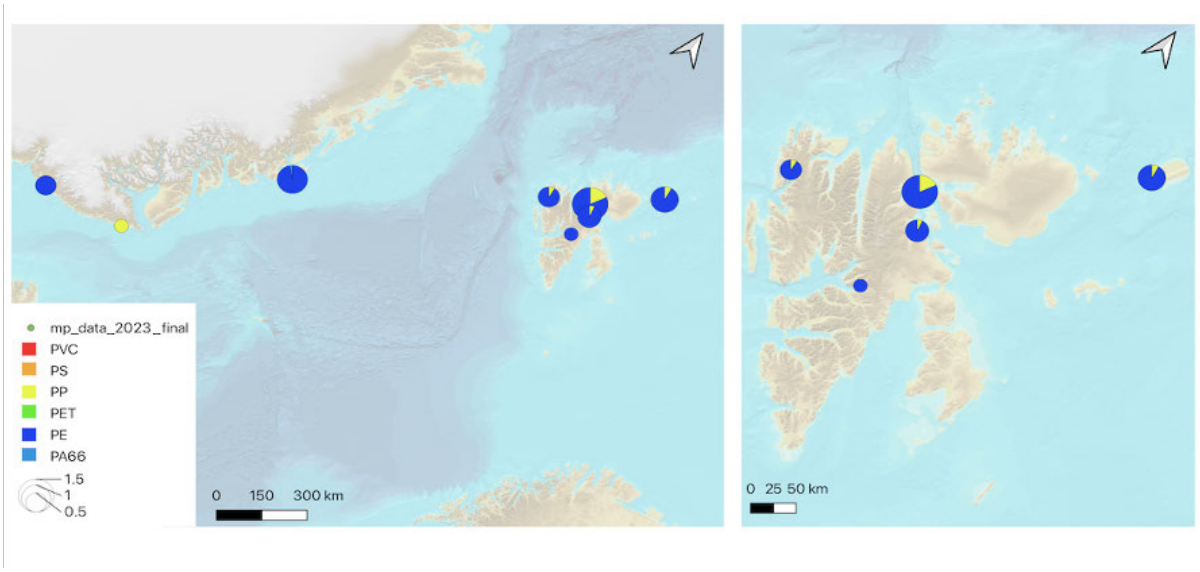

Fig. 16: Spatial distribution of MP particles in Greenland and Svalbard in 2023, visualizing distribution, abundance, and polymer type of net-collected microplastics. The right-hand panel shows a zoomed in view around Svalbard. MP abundance is shown by the symbol size (note that these are log-scaled, i.e., circle size 1 = 10 MP particles km^{-2}).

4.5 Science communication

4.5.1 Popular science articles

The EU4OceanObs ocean observing awareness campaign wants to raise awareness on the need for sustained and comprehensive in situ observations in the Arctic to improve our knowledge of this highly remote area and to better predict its future changes. Within the context of this communication campaign, EU4OceanObs contracted the professional photographer and videographer Xavier Boymond to accompany the science team of the GOOD-IMDOS project during their 2023 expedition onboard the *Charcot.*

As part of the science team on board, Xavier Boymond documented all science activities from preparation of instruments to sampling procedures, sample processing, measurements and data analysis. In addition, he recorded several interviews with the scientists on board giving exclusive insights in their research and personal experience in the field of opportunity science on the *Charcot.*

Based on the collected footage and individual exchanges after the cruise, the science journalist Kira Coley wrote a series of articles, illustrated by visuals from the photographer Xavier Boymond (Table 4). The articles tell a story about the joint European efforts to observe ongoing changes in the Arctic, within the context of the multi-year GOOD-IMDOS project in close partnership with PONANT Science. Through the articles, readers will be able to journey out into the Arctic and understand some of the biggest challenges that this vulnerable yet critical ecosystem for our planet is facing as well as the difficulties of such scientific undertakings. The audience will also get a first-hand impression from scientists involved and get acquainted with some of the human faces and diversity of profiles behind Arctic Ocean observation and science in the EU.

Table 4: List of articles published including their respective URL.

Title	**URL**
Ocean Observing Awareness Campaign Part 3: Arctic Ocean Observing	https://www.eu4oceanobs.eu/oceanobserving-awareness/arctic-observing
Breaking Ice and Barriers: A Tale of Partnership, Preservation, and Promise	https://www.eu4oceanobs.eu/wp-content/uploads/2023/11/Article-1_General-Arctic-Ecosystem_EU4OceanObs.pdf
Beneath the Arctic Ice: The Subtle Ebb of Ocean Oxygen	https://www.eu4oceanobs.eu/wp-content/uploads/2023/11/Article-2_Oxygen_EU4OceanObs.pdf

From Ocean to Ice: Tracking Plastic Pollution in the Arctic	https://www.eu4oceanobs.eu/wp-content/uploads/2023/11/Article-3-Marine-Plastic.pdf
A World Under Ice: How Plankton Shapes Life in a Secluded Arctic Village	https://www.eu4oceanobs.eu/wp-content/uploads/2023/11/Article-4-Plankton-Arctic-EU4OceanObs.pdf
Innovative Alliances: The Transformative Impact of Science-Industry Partnerships	https://www.eu4oceanobs.eu/wp-content/uploads/2024/02/Article-5-Partnerships.pdf

5. Data availability

Table 5: Data and sample storage including the corresponding contact person.

Type	Database	Availability	Free Access	Contact
CTD hydrography (raw data)	OSIS	06/2023	1/2025	aoschlies@geomar.de
Dissolved O_2 O_2 saturation	OSIS	06/2023	1/2025	aoschlies@geomar.de
Chlorophyll *a*	OSIS	06/2023	1/2025	aoschlies@geomar.de
TPC and TPN	OSIS	06/2023	1/2025	aoschlies@geomar.de
Mesozooplankton and particles (UVP)	EcoTaxa	06/2023	1/2025	jtaucher@geomar.de
Microplastic concentration and polymer type	EMODnet	06/2023	1/2025	ajbeck@geomar.de

6. Science team

The science team of the project GOOD-IMDOS in 2023 consisted of the lead scientists and marine biogeochemist Dr. Tim Boxhammer, the technician in marine science Kerstin Nachtigall and the biology student Deborah Stoll (Fig. 17). The Science team was accompanied by the photographer and videographer Xavier Boymond and supported by the science coordinator Geoffroy de Kersauson.

Fig. 17: Scientific team of the cruise. From left to right: Deborah Stoll, Science Coordinator Geoffroy de Kersauson, Tim Boxhammer, Kerstin Nachtigall. Not shown: Xavier Boymond. Photo credit: Xavier Boymond.

The on-board tasks of the science team and Xavier Boymond as well as their profession, early career status and affiliations are listed in Table 6.

Table 6: Science team of the cruise including their profession, early career status, gender, affiliation and tasks on board. The Science team was accompanied by the photographer and videographer Xavier Boymond.

#	Name	Profession	Early career (Y/N)	Affiliation	On-board tasks
1	Dr. Tim Boxhammer	Marine biogeochemist	N	GEOMAR[1]	Lead scientist, CTD, UVP camera system, interviews
2	Kerstin Nachtigall	Technician in marine science	N	GEOMAR[1]	Oxygen concentration, particulate organic material, phytoplankton pigments, interviews
3	Deborah Stoll	Biology student	Y	GEOMAR [1]	Micro- and marcroplastic, interviews
4	Xavier Boymond	Photographer and videographer	N	Under contract by MERCATOR OCEAN[2]	Photo and video documentation

[1] GEOMAR Helmholtz Centre for Ocean Research Kiel (Germany)

[2] MERCATOR OCEAN INTERNATIONAL (France)

7. Acknowledgements

Acknowledgements to PONANT, the crew of *Le Commandant Charcot* and the Science Coordinators at PONANT. Acknowledgements to the EU project ARICE, EU grant agreement No. 730965. Acknowledgments to MERCATOR Ocean International who contracted Xavier Boymond and allowed to perform valuable outreach activities in the Arctic.

We greatly appreciate the assistance on all fronts from the ship's crew, especially the captain and chief engineer as well as the nature guides of PONANT. This work would not have been possible without the enthusiastic and tireless efforts and expertise of the ship's science coordinator, Geoffroy de Kersauson. Financial travel support for this work was provided by PONANT Science, while funding for sample analyses was provided by GEOMAR Helmholtz Centre for Ocean Research Kiel.

8. References

Arístegui, J. and Harrison, W. G.: Decoupling of primary production and community respiration in the ocean: implications for regional carbon studies, Aquat. Microb. Ecol., 29, 199–209, 2002.

Bach, L. T., Paul, A. J., Boxhammer, T., von der Esch, E., Graco, M., Schulz, K. G., Achterberg, E., Aguayo, P., Arístegui, J., Ayón, P., Baños, I., Bernales, A., Boegeholz, A. S., Chavez, F., Chavez, G., Chen, S.-M., Doering, K., Filella, A., Fischer, M., Grasse, P., Haunost, M., Hennke, J., Hernández-Hernández, N., Hopwood, M., Igarza, M., Kalter, V., Kittu, L., Kohnert, P., Ledesma, J., Lieberum, C., Lischka, S., Löscher, C., Ludwig, A., Mendoza, U., Meyer, J., Meyer, J., Minutolo, F., Ortiz Cortes, J., Piiparinen, J., Sforna, C., Spilling, K., Sanchez, S., Spisla, C., Sswat, M., Zavala Moreira, M., and Riebesell, U.: Factors controlling plankton community production, export flux, and particulate matter stoichiometry in the coastal upwelling system off Peru, Biogeosciences, 17, 4831–4852, https://doi.org/10.5194/bg-17-4831-2020, 2020.

Barlow, R. G., Cummings, D. G., and Gibb, S. W.: Improved resolution of mono- and divinyl chlorophylls a and b and zeaxanthin and lutein in phytoplankton extracts using reverse phase C-8 HPLC, Mar. Ecol. Prog. Ser., 161, 303–307, https://doi.org/10.3354/meps161303, 1997.

Beck, A. J., Kaandorp, M., Hamm, T., Bogner, B., Kossel, E., Lenz, M., ... & Achterberg, E. P. (2023). Rapid shipboard measurement of net-collected marine microplastic polymer types using near-infrared hyperspectral imaging. Analytical and Bioanalytical Chemistry, 1-10.

Gerdts, G. (2018). Defining the baselines and standards for microplastics analyses in European waters!?: highlights and pitfalls of JPI-O BASEMAN. In MICRO 2018. Fate and Impact of Microplastics: Knowledge, Actions and Solutions (p. 88). MSFS-RBLZ.

Hamner, W. M., & Schneider, D. (1986). Regularly spaced rows of medusae in the Bering Sea: Role of Langmuir circulation 1. Limnology and Oceanography, 31(1), 171-176.

Paul, A. J., Bach, L. T., Schulz, K.-G., Boxhammer, T., Czerny, J., Achterberg, E. P., Hellemann, D., Trense, Y., Nausch, M., Sswat, M., and Riebesell, U.: Effect of elevated CO_2 on organic matter pools and fluxes in a summer Baltic Sea plankton community, Biogeosciences, 12, 6181–6203, https://doi.org/10.5194/bg-12-6181-2015, 2015.

Pedregosa, F., Varoquaux, G., Gramfort, A., Michel, V., Thirion, B., Grisel, O., ... & Duchesnay, É. (2011). Scikit-learn: Machine learning in Python. the Journal of machine Learning research, 12, 2825-2830.

Picheral 2021 - The Underwater Vision Profiler 6- an imaging sensor of particle size spectra and plankton, for autonomous and cabled platforms

Sharp, J. H.: Improved analysis for “particulate” organic carbon and nitrogen from seawater, Limnol. Oceanogr., 19, 984–989, 1974.

Spreen, G.; Kaleschke, L. and Heygster, G. (2008), Sea ice remote sensing using AMSR-E 89 GHz channels J. Geophys. Res.,vol. 113, C02S03, doi:10.1029/2005JC003384.

Thorpe, S. A. (2009). Spreading of floating particles by Langmuir circulation. Marine Pollution Bulletin, 58(12), 1787-1791.

Van der Walt, S., Schönberger, J. L., Nunez-Iglesias, J., Boulogne, F., Warner, J. D., Yager, N., ... & Yu, T. (2014). scikit-image: image processing in Python. PeerJ, 2, e453.

Van Sebille, E., Aliani, S., Law, K. L., Maximenko, N., Alsina, J. M., Bagaev, A., ... & Wichmann, D. (2020). The physical oceanography of the transport of floating marine debris. Environmental Research Letters, 15(2), 023003.